Talanta 81 (2010) 1766–1771

Contents lists available at ScienceDirect

Talanta

journal homepage: www.elsevier.com/locate/talanta

Ionic liquids: Determination of their aqueous content using differential scanning calorimeter equipment, chaotic parameters and a radial basis network model

José S. Torrecilla*, Ester Rojo, Juan C. Domínguez, Francisco Rodríguez

Department of Chemical Engineering, Faculty of Chemistry, University Complutense of Madrid, Avda. Complutense s/n, 28040 Madrid, Spain

ARTICLE INFO

Article history:
Received 7 September 2009
Accepted 19 March 2010
Available online 25 March 2010

Keywords:
Fractal dimension
Liapunov exponent
Auto correlation coefficient
1-Butyl-3-methylimidazolium bis(trifluoromethylsulfonyl) imide
1-Butyl-3-methylimidazolium hexafluorophosfate
1-Ethyl-3-methylimidazolium bis(trifluoromethylsulfonyl) imide
Water content

ABSTRACT

A new computerized approach to the determination of water in 1-butyl-3-methylimidazolium bis(trifluoromethylsulfonyl) imide, 1-butyl-3-methylimidazolium hexafluorophosfate and 1-ethyl-3-methylimidazolium bis(trifluoromethylsulfonyl) imide ionic liquids (ILs) using the differential scanning calorimeter (DSC) scans of their mixtures with water is presented here. This approach consists of a combination of chaotic algorithms and a radial basis network (RBN). The data collected (heat flow signal) from DSC scans of ILs and water mixtures are used to calculate six chaotic parameters (two Liapunov exponents, two correlation parameters and two fractal dimensions), and then, these values are transferred into an RBN trained computer for modeling and estimating output. The predicted results using the RBN were compared with the measurements of water content carried out by the Karl Fischer technique and the difference between the real and predicted values was less than 0.05 and 4.9% in the internal and external validation, respectively. Such an integrated chaotic parameters (CPs)/RBN system is capable of detecting and quantifying water content in the aforementioned ILs, based on the created models and patterns, without any previous knowledge of this thermal process.

© 2010 Elsevier B.V. All rights reserved.

1. Introduction

Ionic liquids (ILs) are chemicals composed of an organic cation and an inorganic or organic anion. Because of their different natures, ILs exhibit mixed inorganic and organic characters [1]. In addition, ILs can be tailormade for specific purposes by careful selection of their ions [2–4]. Given these two characteristics, these chemicals have shown successful results and great promise in a plethora of applications [5,6]. Their wide industrial applicability means that the knowledge of their physicochemical characteristics is essential. Because of this, currently, one of the broadest research lines consists of determining their most important features (density, viscosity, thermal properties, *etc.*). However, little attention has been paid to the characterization of the purity of these compounds, which has ultimately led to non-reproducible data in the literature [7].

Due to the notable influence of the presence of chemical impurities on the physicochemical properties of ILs [8,9], a reliable and fast method to detect these undesirable compounds is required. The fact that the concentration of minute impurities may generate an essential change in the physicochemical properties of the ionic liquids leads us to believe that this alteration could be based on its chaotic nature. In a recent paper, a chaotic character was detected in the thermal degradation of ionic liquids using a thermogravimetric analyzer (TGA) and differential scanning calorimeter (DSC) apparatus [10]. As a continuation of that work, this chaotic dynamic of the thermal process previously found has been applied here to design a detector of the most common impurity present in ionic liquids, water. In particular, a chaotic tool has been designed here to detect water in three hydrophobic ionic liquids *viz.* 1-butyl-3-methylimidazolium bis(trifluoromethylsulfonyl) imide ([bmim][Tf_2N]), 1-butyl-3-methylimidazolium hexafluorophosfate ([bmim][PF_6]) and 1-ethyl-3-methylimidazolium bis(trifluoromethylsulfonyl) imide ([emim][Tf_2N]) and two hydrophilic ILs *viz.* 1-ethyl-3-methylimidazolium ethylsulfate ([emim][$EtSO_4$]) and 1-butyl-3-methylimidazolium methylsulfate ([bmim][$MeSO_4$]) by differential scanning calorimeter apparatus.

2. Material and methods

2.1. Reagents, solutions and instrumentation

In this work, 1-butyl-3-methylimidazolium bis(trifluoro methylsulfonyl) imide, 1-butyl-3-methylimidazolium hexafluorophosfate and 1-ethyl-3-methylimidazolium ethylsulfate bis(trifluoromethylsulfonyl) were used. These three ILs all present

* Corresponding author. Tel.: +34 91 394 42 40; fax: +34 91 394 42 43.
E-mail address: jstorre@quim.ucm.es (J.S. Torrecilla).

0039-9140/$ – see front matter © 2010 Elsevier B.V. All rights reserved.
doi:10.1016/j.talanta.2010.03.026

Table 1
Operating conditions of DSC experiments.

Operating conditions	DSC
ILs used	[bmim][Tf_2N] [bmim][PF_6] [bmim][$MeSO_4$] [emim][$EtSO_4$] [emim][Tf_2N]
Temperature range (K)	123.15–303.15
Initial weight range of sample (mg)	9–21
Dry N_2 flow (mL min^{-1})	50
Heating rate (K min^{-1})	10
Volume of pans (μL)	120

a purity higher than 99% and these have been supplied by *io-li-tec*. In addition, 1-ethyl-3-methylimidazolium ethylsulfate ionic liquid ([emim][$EtSO_4$], ≥95% purity, from Sigma-Aldrich Chemie GmbH, water content was 2000 ppm), and 1-butyl-3-methylimidazolium methylsulfate ([bmim][$MeSO_4$] ≥95% purity, from Sigma-Aldrich Chemie GmbH, water content was 1000 ppm) were also used. All the ionic liquid samples used were previously dried by heating at 60 °C for 24 h under reduced pressure. The mean of three replicate measurements was reported.

Other non-ionic liquids compounds acquired by Panreac Chimie S.A.R.L. *viz*. lithium chloride (LiCl ≥ 99%), potassium acetate ($CH_3COOK \geq 99\%$), magnesium chloride 6-hydrate ($MgCl_2 \cdot 6H_2O \geq 99\%$), potassium carbonate ($K_2CO_3 \geq 99\%$), sodium dichromate 2-hydrate ($Na_2Cr_2O_7 \cdot 2\,H_2O \geq 99.5\%$), sodium bromide (BrNa ≥ 99%), sodium nitrite ($NaNO_2 \geq 98\%$), sodium chloride (NaCl ≥ 99.95%) have been used. For volumetric Karl Fischer titration, methanol dry (CH_3OH, Riedel-de Haën, HYDRANAL-water mass fraction < 0.01%) and standard (Riedel-de Haën, HYDRANAL-standard (5.00 ± 0.02) mg mL^{-1} as water) were used. The aqueous solutions were prepared using ultra pure water obtained from a Milli-Q water purification system (Millipore, Saint Quentis Yvelines, France).

The measurements of the heat flow associated with material transitions as a function of temperature were carried out on a Mettler Toledo DSC821^e. The differential scanning calorimeter equipment was calibrated according to the temperature range used and the manufacturer's instructions [11]. The temperature measurements were carried out with an accuracy of ±0.1 K. The experimental conditions and chemicals used to design, optimize and test the linear and non-linear models are shown in Table 1. In every experiment, stainless steel pans with a volume of 120 μL and a purge flow of 50 mL min^{-1} of dry nitrogen were used. The temperature range was between 123.15 and 303.15 K, whereas the heating/cooling rate was fixed at 10 K min^{-1} [12].

2.1.1. Hydration equipment

In order to input water into the ILs, an isopiestic method was used [13]. Several runs were carried out in air with different relative humidity values which were generated by saturated solutions of different salts in water at 298.15 K and at atmospheric pressure (Table 2). The experimental device consists of a cylindrical glass vessel half filled with a saturated salt solution at 298 K [9]. The type of salt resulted in a known equilibrium air humidity inside the device. A small cubic container made of glass was filled with IL and hung at the top of the vessel. The container was periodically weighed until the mass remained constant. The IL was hydrated until the relative change of the water content rate (WCR, Eq. (1)) between two consecutive mass measurements of the container was ≤0.03%.

$$\mathrm{WCR} = \frac{Ms(t+1) - Ms(t)}{t \cdot Mso} \times 100 \quad (1)$$

Table 2
Air equilibrium relative humidities of saturated salt solutions at T = 298.15 K [13].

Chemical	Relative humidity (%)
Lithium chloride	11.1
Potassium acetate	22.5
Magnesium chloride 6-hydrate	32.5
Potassium carbonate	43.7
Sodium dichromate 2-hydrate	53.3
Sodium bromide	58.1
Sodium nitrite	64.4
Sodium chloride	75.4

where *Mso*, *Ms* and *t* are the initial sample mass, sample mass and the hydration time in hours, respectively. The operating procedure consisted of placing 15 cm^3 of IL in a small closed vessel in which the relative humidity (RH) is controlled by the saturated salt solutions (25 cm^3). After 5 days, it was verified that the equilibrium between the water vapour and the IL (WCR < 0.03%) had been reached. In this way, eight different unsaturated solutions of IL in water were made. The hydration equipment was cleaned between experiments by rinsing with acetone and water, followed by drying in an oven at 333.15 K for 24 h [9].

Water content of every hydrated ionic liquid was measured by a Karl Fischer titrator DL31 from Mettler Toledo and using the one-component technique. The polarising current for potentiometric end-point determination was 20 A and the stop voltage 100 mV. The end-point criterion was the drift stabilisation (3 μg H_2O min^{-1}) or maximum titration time (10 min). The measurement was corrected for the baseline drift, defined as the residual or penetrating water that the apparatus removes per minute. The expanded uncertainty decreases with the mass fraction of water; at 3×10^{-2}, 6×10^{-2}, and 9×10^{-2} the uncertainty decreases by 2.5%, 0.6% and 0.4%, respectively.

2.2. Chaotic parameters used

To check the chaotic nature of the thermal processes and their relation with the presence of water in the three ILs studied, six chaotic parameters have been calculated using DSC scans of mixtures composed of water and IL.

2.2.1. Liapunov exponents (LEs)

Liapunov exponents (LEs) characterize the dynamics of a complex process and quantify the average growth of infinitesimally small errors at initial points. LE values characterize the rate of separation of infinitesimally close trajectories. This can be used to measure the sensitivity of a system's behaviour to initial conditions [14]. The LE parameter has been calculated by Eq. (2).

$$\mathrm{LE} = \frac{1}{\Delta t_m} \sum_{k=1}^{m} \log_2 \frac{L(t_k)}{L(t_{k-1})} \quad (2)$$

where Δt_m and $L(t_k)$ are the prediction time interval and the distance between the developed points in the phase space, respectively. This parameter is one of the most sensitive to determine chaotic dynamic. Depending on the sign of the maximal LE (MLE), different types of attractors (dynamical systems evolve after a long period of time) can be found. MLE < 0 represent stable fixed, MLE = 0 or MLE = ∞ imply stable limit cycle or noise, respectively, and 0 < MLE < ∞ implies chaos, which means that neighboring points of trajectories in the phase space diverge [15].

2.2.2. Autocorrelation functions (AFc(k)) and correlation (AF(k))

These parameters measure linearly how strongly on average each data point is correlated with one *k* time steps away, Eqs. (3) and (4), respectively. They are the ratio of the autocovariance to

the variance of the data. In general, AF(k) and $R^2(k)$ are between 1 (small k) and 0 (large k) [16].

$$\mathrm{AFc}(k) = \frac{\sum_{n=1}^{N-k}(X_n - \bar{X})(X_{n-k} - \bar{X})}{\sum_{n=1}^{N-k}(X_n - \bar{X})^2} \quad (3)$$

$$\mathrm{AF}(k) = \frac{\sum_{n=1}^{N-k}(X_n - \bar{X})(X_{n-k} - \bar{X})}{\sqrt[z]{\sum_{n=1}^{N-k}(X_n - \bar{X})^2 \sum_{n=1}^{N-k}(X_{n-k} - \bar{X})}} \quad (4)$$

where X, $\bar{X}$ and N represent the dataset of the measurements by DSC equipment, their average and the total number of datasets, respectively. Given that the k value was assumed equal to 1 min, throughout the paper AFc(k) and AF(k) have been referred to as AFc and AF, respectively.

2.2.3. Fractal dimension

Fractal dimension, in general, is a number that quantitatively describes how an object fills its space. In plane geometry, objects are solid and continuous and given that they have no holes, they have integer dimensions. Fractals are rough and often discontinuous, and so, they present non-integer dimensions. From a fractal geometry point of view, the fractal dimension is a measure of complexity that is used to describe the irregular nature of lines, curves, planes or volumes. In this work, the regularization dimension (RD) and the box dimension (BD) using a plain box method have been computed by Fraclab version 2.0 (Toolbox of Matlab version 7.01.24704, R14) [17]. Considering the original signal as fractal, its graph will have an infinite length. Taking into account RD and that all regularized versions have a finite length, the RD measures the speed at which this convergence to the infinite takes place. To calculate BD, the software works exactly in the same way as when computing the regularization dimension except that in this case different box sizes are tested. In almost all cases, the estimation of fractal dimension by the box method is less accurate than the calculation by the regularization method. All necessary parameters values to calculate RD and BD were selected by default configuration settings of the software used [17].

2.3. Learning, verification and validation sample

Every dataset of the learning and verification samples is composed of six aforementioned chaotic parameters with their respective water content in ppm. These parameters are calculated from the DSC scans of two hydrophobic ionic liquids *viz.* [bmim][Tf_2N] and [bmim][PF_6] with different water concentrations. As an example, DSC scans of six mixtures composed of [bmim][PF_6] and water content are shown in Fig. 1. Using the hydratation equipment, each ionic liquid has been artificially contaminated with 20 different water concentrations and in all cases, three replicate measurements of DSC scan for each sample were carried out. The only difference between the verification and learning samples is that the latter is composed of 80% (96 datasets) of data and the former of the remaining 20% (24 datasets). Taking into account that every datum of the verification sample should be interpolated within learning range, the data were randomly distributed between both samples.

The above mentioned chaotic parameters have been calculated using different DSC scans from a hydrophobic IL [emim][Tf_2N] and two hydrophilic ionic liquids *viz.* [emim][$EtSO_4$] and [bmim][$MeSO_4$] ILs [12]. Using these chaotic parameters and their respective water content, two different external validation samples have been made. The first and the second are composed of the results achieved using the hydrophobic ionic liquid ([emim][Tf_2N]), and both hydrophilic ILs ([emim][$EtSO_4$] and [bmim][$MeSO_4$]), respectively. These two external validation samples present the same format as the learning and verification samples.

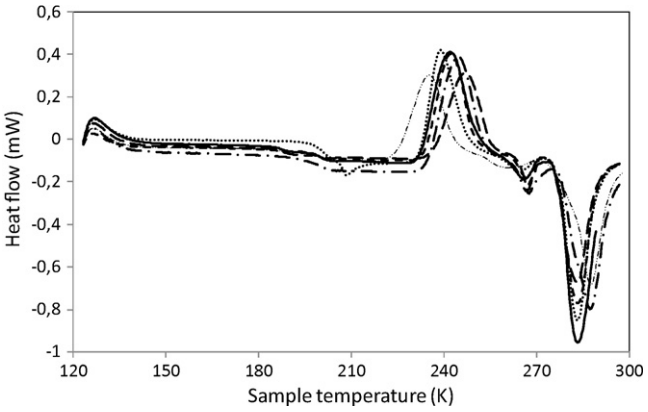

Fig. 1. DSC scans of [bmim][PF_6] with 2439.40 (–···–), 3841.23 (–·–), 6361.51 (– –), 8112.47 (- - -), 9950.96 (· · ·) and 11929.80 (—) ppm of water (exothermic up).

2.4. Radial basis network model

The radial basis model consists of three layers: the input, hidden radial basis and output. The input layer has no calculation power and serves as an input distributor to the hidden radial basis layer. The net input to the hidden radial basis neuron is the vector distance between its weight vector (self-adjustable parameter of the net), w, and the input vector, p, multiplied by the bias. The transfer function of radial basis neurons is a Gaussian function, Eq. (5). The radial basis function has a maximum of 1 when its input is 0. As the distance between w and p decreases, the output increases. The bias allows the sensitivity of the radial basis neuron to be adjusted. The operation of the output layer is a linear combination of the radial basis units according to Eq. (6) [18].

$$G_j(x) = \frac{1}{e^{x^2}} \quad (5)$$

$$y_k(x) = \sum_{j}^{n_h} w_{jk} \cdot G_j(x) + w_k \quad (6)$$

In Eqs. (5) and (6), y_k is the kth output unit for the input vector x, n_h is the number of hidden radial basis units, w_{jk} is the weight between the jth hidden and the kth output neurons, G_j is the notation for the output of the jth radial basis unit, and w_k is the bias. A radial basis model (RBN) called radial basis networks exact fit was used in this work. The RBN algorithm rapidly designs a radial basis network with zero error on the design vectors, and depends on a matrix of input vectors, a matrix of target class vectors and a spread of radial basis functions commonly called spread constant. This is a parameter related to the average distance between any two inputs. As the spread constant was the only parameter to be optimized, it was selected after trying more than 150 values and choosing the best. The spread constant was analysed taking into account that the estimations should be carried out using the lowest possible mean prediction error (MPE), Eq. (7).

$$\mathrm{MPE} = \frac{1}{N}\sum_{n}\frac{|r_n - y_n|}{r_n} \times 100 \quad (7)$$

In Eq. (7), N, y_n and r_n, are the number of observations, model estimation and real value, respectively [18,19].

Table 3
Chaotic parameters from DSC scans of ionic liquids.

IL	WC (ppm)	LTi	LTe	AF	AFc	RD	BD
[bmim][PF_6]	2439.4	2.8995×10^{-8}	4.2246×10^{-5}	0.5789	0.5211	1.2935	0.8682
	3841.2	3.4624×10^{-8}	3.6228×10^{-5}	0.5660	0.5347	1.3080	0.8699
	6361.5	4.7035×10^{-8}	5.3323×10^{-5}	0.4794	0.5696	1.3145	0.8704
	8112.5	4.5152×10^{-8}	4.8651×10^{-5}	0.4309	0.5415	1.3190	0.8718
	9951.0	5.3592×10^{-8}	4.9902×10^{-5}	0.4195	0.5768	1.3266	0.8735
	11929.8	5.3654×10^{-8}	6.3402×10^{-5}	0.4154	0.6563	1.3336	0.8782
[bmim][Tf_2N]	1498.9	2.0044×10^{-9}	6.1969×10^{-5}	0.7014	0.5723	1.2710	0.8565
	2007.0	2.0234×10^{-9}	6.9662×10^{-5}	0.4356	0.4177	1.2927	0.8506
	2587.4	2.4021×10^{-9}	6.9756×10^{-5}	0.3407	0.3799	1.3123	0.8477
	3335.8	5.2187×10^{-9}	7.0348×10^{-5}	0.3072	0.3245	1.3083	0.8463
	4313.6	8.6435×10^{-9}	7.1197×10^{-5}	0.3014	0.2723	1.3151	0.8465
	4753.2	1.8753×10^{-8}	7.3220×10^{-5}	0.2682	0.2490	1.3188	0.8411
	5503.2	2.4657×10^{-8}	7.4461×10^{-5}	0.2311	0.2387	1.3311	0.8359
	5985.6	3.0598×10^{-8}	7.5324×10^{-5}	0.2066	0.2238	1.3490	0.8311
[emim][Tf_2N]	1503.3	8.4774×10^{-9}	2.3945×10^{-6}	0.5804	0.2996	1.2836	0.8483
	2792.9	1.0960×10^{-8}	2.8630×10^{-6}	0.5510	0.2620	1.2922	0.8461
	3946.0	1.4075×10^{-8}	3.4646×10^{-6}	0.5199	0.2503	1.2923	0.8433
	5254.1	1.2874×10^{-8}	1.4876×10^{-6}	0.5295	0.2383	1.2975	0.8420
	6881.8	8.6731×10^{-9}	1.7460×10^{-6}	0.4623	0.2357	1.2962	0.8412
	7981.8	1.4888×10^{-8}	1.0299×10^{-5}	0.4211	0.2246	1.2965	0.8420
	9089.0	1.9213×10^{-8}	1.9965×10^{-5}	0.3489	0.2235	1.2982	0.8405
	10552.6	3.5702×10^{-8}	2.0108×10^{-5}	0.3345	0.2050	1.3062	0.8379
[emim][$EtSO_4$]	470	2.3956×10^{-9}	3.4874×10^{-6}	0.2174	0.2097	1.2725	0.8411
[bmim][$MeSO_4$]	1018	2.3966×10^{-9}	2.4746×10^{-9}	0.3550	0.2637	1.2598	0.8588

3. Results and discussion

A database form by water content, Liapunov exponent with respect to time and temperature, correlation coefficient, autocorrelation coefficient and two fractal dimensions were made. In the first study, in every IL case, a linear model has been proposed. The second consists of a linear and non-linear models to study the purity of all ILs tested.

3.1. Chaotic parameters

Three different types of chaotic parameters have been calculated *viz*. Liapunov exponents, correlation parameters and fractal dimensions.

3.1.1. Liapunov exponent

This exponent characterizes the dynamic of process and the separation of infinitesimally close trajectories. In addition, it can evaluate the sensitivity of the system with respect to the initial conditions. Given that Liapunov exponents with respect to time (LTi) and with respect to temperature (LTe) are non-integer and positive, Table 3, these describe some different strange attractors, whose trajectories appear to skip around randomly.

3.1.2. Autocorrelation functions (AFc) and correlation (AF) coefficients

Considering that the correlation coefficient equal to unity means that the property is constant in time t with respect $t-k$ (k = 1 min), and the average of correlating and autocorrelating parameters are 0.43 (ranged 0.7 and 0.21) and 0.37 (ranged 0.66 and 0.2), respectively, the variation of heat flow during 1 min could in part represent the chaotic dynamic of this process. Correlation function for the heat flow of [bmim][PF_6] IL with a water content of 2439.4 and 11929.8 ppm measured by DSC equipment is shown in Fig. 2.

3.1.3. Fractal dimensions

The RD and BD parameters define the output signals tortuosity and these are a measure of complexity that is used to describe the irregular nature of curves. In all ILs cases, the mean RD and BD values with respect to the concentration of water are, respectively, between 1.31 (range 1.35 and 1.27) and 0.85 (range 0.88 and 0.83), Table 3. There is a mathematical relation between the water content of the ILs studied and RD and BD parameters values. That is, the correlation coefficient of real water content, and those linearly estimated using RD and BD values range between 0.815 and 0.955, and 0.875 and 0.907, respectively.

3.2. Linear models

To quantify the water concentration present in the ionic liquids tested using the easiest way possible, a simple global linear model was designed, Table 4. In the best case, using LTi as the only independent variable, the global model is able to estimate the water content of three ILs with a correlation coefficient higher than 0.506 and a mean prediction error (MPE) less than 40.54%, Eq. (7). In the light of these results, these models are inadequate.

Therefore, depending on the chaotic parameters and IL used, different simple linear regression models have been tested, Table 5. In the case of [bmim][PF_6], [bmim][Tf_2N] and [emim][Tf_2N] ILs the best models are achieved using RD ($R^2 > 0.955$), BD ($R^2 > 0.907$) and

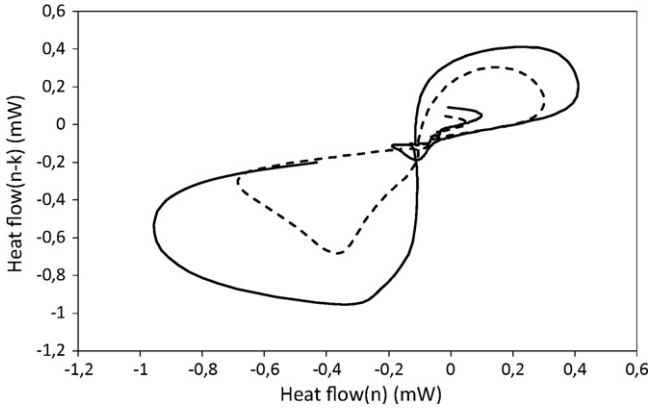

Fig. 2. Correlation function for the heat flow of [bmim][PF_6] IL and 2439.4 (- - -) and 11929.8 ppm (—) of water content measure by DSC equipment (k = 1 min).

Table 4
Global linear models to estimate the water content (WC) in all ionic liquids tested.

Global linear model	R^2	Error (%)
$WC = 1.29 \times 10^{11} \cdot LTi - 2.66 \times 10^3$	0.506	40.54
$WC = -8.20 \times 10^6 \cdot LTe - 5.83 \times 10^3$	0.006	69.28
$WC = -8.82 \times 10^3 \cdot AF + 9.26 \times 10^3$	0.136	58.71
$WC = 1.56 \times 10^3 \cdot AFc + 4.91 \times 10^3$	0.006	69.94
$WC = 2.19 \times 10^4 \cdot RD - 3.09 \times 10^4$	0.470	46.03
$WC = 3.94 \times 10^4 \cdot BD - 2.80 \times 10^4$	0.033	69.86

AF ($R^2 > 0.943$), respectively. Although at first sight, these models could be adequate, their MPE values are less than 8.1, 11.4 and 15.9% and signify that these models are unsuitable to estimate water content in the ILs studied.

Trying to find the best linear model, more than 128 multiple regression models were tested. Taking into account the statistical results, the best model, in which the linear combination of all six independent variables (both Liapunov exponents, both correlation functions and both fractal dimensions) was used, is shown in Eq. (8). Due to the MPE being close to 29%, this model is also inadequate. Because of this, a non-linear model has been tested.

$$WC = 3.104 \times 10^5 + 1.095 \times 10^{11}\,\mathrm{LTi} - 1.318 \times 10^8\,\mathrm{LTe} - 3.891 \times 10^4\,\mathrm{AF} + 3.919 \times 10^4\,\mathrm{AFc} - 7.639 \times 10^4\,\mathrm{BR} - 2.344 \times 10^5\,\mathrm{BD}\,(R^2 > 0.851;\ \mathrm{MPE} = 28.7\%) \quad (8)$$

3.3. Non-linear model

Considering that the most influential variables of the process to be studied are those selected in the aforementioned multiple regression model (Eq. (8)), and that the water content must be non-linearly estimated, a radial basis network model has been designed.

3.3.1. Optimisation process of the radial basis model

The number of input nodes and output neurons are fixed by the requirements of the system to be modeled. That is, six input nodes (both Liapunov exponents, correlation and autocorrelation functions and two fractal dimensions) and one output neuron (water content of the ILs). The hidden neurons number is optimized by the radial basis network, itself. Then, the only parameter to optimize is the spread constant. This process was carried out by testing different spread constant values between 0.001 and 15 [18]. The response variables were the mean prediction error (MPE), Eq. (7) and correlation coefficient (R^2) (predicted *vs.* experimental values).

Table 6
Parameters of RBN model and statistical results of verification process.

Parameters of RBN model	
Input nodes	6
Output nodes	1
Spread value	1
Statistical results	
Correlation coefficient	>0.99
Mean prediction error (%)	0.05

The design was analyzed taking into account that the estimations should be carried out with the lowest MPE values possible. The optimized spread constant found was equal to unity.

3.3.2. Verification process of the radial basis model

Once the RBN model had been optimized, the verification process was carried out. In this process, the model was tested against the verification sample that had not been included in the RBN learning. In the verification process, the MPE and R^2 values between experimental and estimated by RBN model were calculated (R^2 higher than 0.99 and MPW less than 0.05%), Table 6. In the light of these statistical results, water content of ILs and chaotic parameters studied show a high mathematical dependence.

As was expected, of all the models developed, the RBN model is the most reliable, since it provides a non-linear match between chaotic parameters and water content. Nevertheless, the applicability of this chaotic parameter/RBN approach must be tested in other types of ionic liquids.

3.3.3. Validation process of the radial basis model

Here, two external validation processes have been carried out *viz.* one for a hydrophobic IL ([emim][Tf_2N]) and the other for two hydrophilic ILs ([emim][$EtSO_4$] and [bmim][$MeSO_4$]). That is, the optimized RBN model has been used to estimate the impurity concentration in two different families *viz.* hydrophobic and hydrophilic ionic liquids.

As was expected, the statistical results provided in the estimation of water content of [emim][Tf_2N] (similar to [bmim][Tf_2N] and [bmim][PF_6], which were used in the learning process) are better than those calculated when the water content of [emim][$EtSO_4$] and [bmim][$MeSO_4$] was estimated, Table 7. Comparing the MPE in both validation processes, the MPE using the first validation sample (4.93%) is nearly two times the MPE error using the second validation sample (9.86%). In the light of these results, the RBN model

Table 5
Lineal models to estimate the water content (WC) of each ionic liquid.

	Linear model	R^2	Error (%)
[bmim][PF_6]	$WC = 3.41 \times 10^{11} \cdot LTi - 7.84 \times 10^3$	0.904	12.05
	$WC = 3.25 \times 10^{11} \cdot LTe - 8.81 \times 10^3$	0.705	33.14
	$WC = -4.65 \times 10^4 \cdot AF - 2.95 \times 10^4$	0.907	11.37
	$WC = 6.32 \times 10^4 \cdot AFc - 2.87 \times 10^4$	0.726	30.23
	$WC = 6.06 \times 10^4 \cdot RD - 9.81 \times 10^4$	0.985	8.117
	$WC = 9.63 \times 10^5 \cdot BD - 8.33 \times 10^5$	0.875	21.18
[bmim][Tf_2N]	$WC = 1.36 \times 10^{11} \cdot LTi + 2.14 \times 10^3$	0.876	16.3
	$WC = 3.52 \times 10^{11} \cdot LTe - 2.12 \times 10^4$	0.786	24.29
	$WC = -8.78 \times 10^3 \cdot AF + 6.81 \times 10^3$	0.716	26.94
	$WC = -1.29 \times 10^4 \cdot AFc + 8.06 \times 10^3$	0.856	19.61
	$WC = 1.13 \times 10^4 \cdot RD - 1.48 \times 10^4$	0.823	18.49
	$WC = -1.93 \times 10^5 \cdot BD + 1.67 \times 10^5$	0.907	11.41
[emim][Tf_2N]	$WC = 2.69 \times 10^{11} \cdot LTi + 1.80 \times 10^3$	0.563	47.76
	$WC = 3.23 \times 10^8 \cdot LTe - 3.48 \times 10^3$	0.676	44.08
	$WC = -3.32 \times 10^4 \cdot AF + 2.15 \times 10^4$	0.943	15.99
	$WC = -1.03 \times 10^5 \cdot AFc + 3.10 \times 10^4$	0.885	26.59
	$WC = 7.71 \times 10^4 \cdot RD - 1.20 \times 10^5$	0.899	21.04
	$WC = -9.22 \times 10^4 \cdot BD + 7.83 \times 10^5$	0.890	18.25

Table 7
Estimation of water content (WC) by RBN model and global statistical results of the first and second external validation processes.

Ionic liquid	Real WC	Estimated WC
First external validation process		
[emim][Tf_2N]	1503.3	1590.5
	2792.9	3012.6
	3946.0	3846.5
	5254.1	5546.9
	6881.8	6941.0
	7981.8	7822.6
	9089.0	9200.2
	10552.6	11987.5
Statistical result		
Correlation coefficient		0.984
Mean prediction error (%)		4.930
Second external validation process		
[emim][$EtSO_4$]	470.0	521.9
[bmim][$MeSO_4$]	1018.0	929.6
Statistical result		
Mean predition error (%)		9.863

is only adequate to estimate the water content of other similar ionic liquids to those used in the learning sample. Because of this, similarly to most of the modelization using neural networks, the adequate selection of the ionic liquids that composed the learning sample and the optimization of the operation range is required to improve the determination of this type of impurity.

When thermal processes are being analyzed and the water affects the thermal profile of the chemical studied, this approach is useful to determine "on line" and quantify the concentration of water in a relatively easy way. Obviously, this approach is proposed not to replace the classical technique to measure water content of ionic liquids, but to open an interesting door to determine "on line" the concentration of impurities present in such important chemicals.

4. Conclusion

To determine impurity in ionic liquids, a new computerized approach based on chaotic parameters is presented. Once six chaotic parameters have been calculated using DSC scans of 1-butyl-3-methylimidazolium bis(trifluoromethylsulfonyl) imide, 1-butyl-3-methylimidazolium hexafluorophosfate and 1-ethyl-3-methylimidazolium bis(trifluoromethylsulfonyl) imide ionic liquids with different water concentration values, the aqueous content in these ionic liquids have been estimated by linear (regression models) an non-linear (radial basis network) models. In the latter case, during the verification process, the mean prediction error found was less than 0.05%. When the water content of a similar IL is estimated (first validation sample), this value is increased to 4.930%. When the water content of a completely different IL is estimated the mean prediction error nearly doubles (9.863%). In general, although these results were expected, these lead us to pay more attention to select the most suitable ionic liquids to make a useful database for a given application.

A non-linear mathematical dependence between the chaotic parameters studied and the water content of ionic liquids studied have been found. When thermal processes are being analyzed and the water affects the thermal profile of chemical studied, this CP/RBN approach could be useful to determine the reliability of the thermal measurements. Obviously, this CP/RBN approach does not replace the classical techniques to measure the water content of chemicals, but it opens a door to the "on line" determination of impurities present in such important chemicals as ionic liquids with incipient applications at industrial scale.

Acknowledgement

José S. Torrecilla is supported by a Ramón y Cajal research contract from the "Ministerio de Ciencia e Innovación" in Spain.

References

[1] W. Nelson, Green Solvents for Chemistry: Perspectives and Practice, Oxford University Press, New York, 2003.
[2] J. Palomar, V.R. Ferro, J.S. Torrecilla, F. Rodríguez, Ind. Eng. Chem. Res. 46 (2007) 6041.
[3] J. Palomar, J.S. Torrecilla, V.R. Ferro, F. Rodríguez, Ind. Eng. Chem. Res. 47 (2008) 4523.
[4] J. Palomar, J.S. Torrecilla, V.R. Ferro, F. Rodríguez, Ind. Eng. Chem. Res. 48 (2009) 2257.
[5] N.V. Plechkova, K.R. Seddon, Chem. Soc. Rev. 37 (2008) 123.
[6] D. Wei, A. Ivaska, Anal. Chim. Acta 607 (2008) 126.
[7] A. Stark, P. Behrend, O. Braun, A. Müller, J. Ranke, B. Ondruschka, B. Jastorff, Green Chem. 10 (2008) 1152.
[8] K.R. Seddon, A. Stark, M.J. Torres, Pure Appl. Chem. 72 (2000) 2275.
[9] J.S. Torrecilla, T. Rafione, J. García, F. Rodríguez, J. Chem. Eng. Data 53 (2008) 923.
[10] J.S. Torrecilla, E. Rojo, J.C. Domínguez, F. Rodríguez, Talanta 79 (2009) 665.
[11] J. Schawe, R. Riesen, J. Widmann, M. Schbnell, K. Vogel, U.U. Jorimann, Low temperature calibration, in: UserCom (Information for Users of METTLER TOLEDO Thermal Analysis Systems), vol. 9, METTLER TOLEDO, Schwerzenbach, Switzerland, 1999, pp. 1–4.
[12] A. Fernández, J.S. Torrecilla, J. García, F. Rodríguez, J. Chem. Eng. Data 52 (2007) 1979.
[13] J.S. Torrecilla, J.M. Aragón, M.C. Palancar, Eur. J. Lipid Sci. Technol. 108 (2006) 913.
[14] P.G. Drazin, Nonlinear Systems, Cambridge University Press, Cambridge, United Kingdom, 1992.
[15] H. Kant, T. Schreiber, Nonlinear Timer Series Analysis, Cambridge University Press, Cambridge, 2005.
[16] J.C. Sprott, Chaos and Time-series Analysis, Oxford University Press Inc., New York, 2003.
[17] J.L. Véhel, http://complex.futurs.inria.fr/FracLab/manual.html, 2009.
[18] H. Demuth, M. Beale, M. Hagan, in Neural Network Toolbox for Use with MATLAB® User's Guide. Version 5. Ninth printing Revised for Version 5.1 (Release 2007b); 2007 (online only).
[19] J.S. Torrecilla, M. Deetlefs, K.R. Seddon, F. Rodríguez, Phys. Chem. Chem. Phys. 10 (2008) 5114.